ELSEVIER

Journal of Fluids and Structures 25 (2009) 389–405

JOURNAL OF FLUIDS AND STRUCTURES

www.elsevier.com/locate/jfs

Coupled vibration of a partially fluid-filled cylindrical container with a cylindrical internal body

E. Askari, F. Daneshmand*

Mechanical Engineering Department, School of Engineering, Shiraz University, Shiraz 71348-51154, Iran

Received 29 February 2008; accepted 16 July 2008

Abstract

In the present paper a method is proposed to investigate the effects of a rigid internal body on the coupled vibration of a partially fluid-filled cylindrical container. The internal body is a thin-walled and open-ended cylindrical shell. The internal body is concentrically and partially submerged inside a container. The radial and axial distances between the internal body and the container are filled with fluid. Along the contact surface between the container and the fluid, the compatibility requirement for the fluid–structure interactions is applied and the Rayleigh–Ritz method is used to calculate the natural frequencies and modes of a partially fluid-filled cylindrical container. The fluid domain is continuous, simply connected, and non-convex. The fluid is assumed to be incompressible and inviscid. The velocity potential for fluid motion is formulated in terms of eigenfunction expansions for two distinct fluid regions. The resulting equations are solved by using the Galerkin method. The results from the proposed method are in good agreement with experimental and numerical solutions available in the literature for the partially water-filled cylindrical container without internal body. A finite element analysis is also used to check the validity of the present method for the partially water-filled cylindrical container with internal body. The effects of the fluid level, internal body radius, and internal body length on the natural frequencies of the coupled system are also investigated.

Keywords: Coupled vibration; Fluid–structure interactions; Internal body; Rayleigh–Ritz method; Eigenfunction expansions; Galerkin method

1. Introduction

Dynamic behavior of structures coupled with fluid is of great importance in various scientific and engineering applications, such as fluid-storage tanks, fuel tanks of space vehicles, dam-reservoir systems, nuclear reactors, and tower-like structures (Jadic et al., 1998; Ergin and Temarel, 2002; Biswal et al., 2004; Krishna and Ganesan, 2007). Due to the vibration of the structural surface, the pressure changes which induces reactive forces on the surface and makes the problem complicated. The solution methods for the free-vibration analysis of fluid–structure interaction problems can be classified into two groups, the analytical and numerical methods. In this paper, an analytical method for fluid–structure interaction problems is proposed.

*Corresponding author. Tel.: +98 711 6287508; fax: +98 711 6275028.
E-mail address: daneshmd@shirazu.ac.ir (F. Daneshmand).

0889-9746/$ - see front matter © 2008 Elsevier Ltd. All rights reserved.
doi:10.1016/j.jfluidstructs.2008.07.003

Nomenclature

a	container radius
b	internal body radius
E	Young's modulus
H	fluid level
h	internal body length
$\mathbf{K}_s$	stiffness matrix of the shell
L	container length
$\mathbf{M}_s$	mass matrix of the shell
$\mathbf{M}_L$	mass matrix of the fluid
r, θ, x	longitudinal, circumferential, radial coordinates
$u(x, \theta)$	axial displacement of the shell
$v(x, \theta)$	circumferential displacement of the shell
$w(x, \theta)$	radial displacement of the shell
β_s	eigenvalue of sth mode of a clamped-free beam
λ_m	$(2m-1)(\pi/2H)$
ν	Poisson's ratio
ρ_L	mass density of the fluid
ρ_s	mass density of the shell
$\tilde{\varphi}(r, \theta, x, t)$	velocity potential of the fluid
$\varphi^{\mathrm{I}}(r,\theta,x)$	deformation potential in region (I)
$\varphi^{\mathrm{II}}(r,\theta,x)$	deformation potential in region (II)
$\psi_s(x)$	beam eigenfunction associated with eigenvalue β_s
ω	circular frequency

Numerous research on fluid–structure interaction problems have been conducted by different analytical approaches such as the eigenfunction expansion method (Kondo, 1981), the Galerkin method (Cheung and Zhou, 2002; Yamaki et al., 1984), the Rayleigh quotient method (Zhu, 1994), the Rayleigh–Ritz method (Zhu, 1995; Amabili, 1996, 1997a; Amabili et al., 1998; Jeong, 2006), the collocation method (Mikami and Yoshimura, 1992), and the Fourier series expansion method (Bauer and Komatsu, 1994; Jeong and Lee, 1998).

Analytical methods are not efficient in studying fluid–structure interaction problems when the system is complex. A class of such problems involves structures with more than one component. Thus, when the solid coupled with the fluid is composed of simple components (substructures), a good idea is to use a method for synthesizing the substructures. A particularly suitable approach for this purpose is the use of artificial springs, simulating the junctions between the substructures. This technique is applied to model the structures coupled with fluid by Amabili (1997a, b).

A different class of complex problems involves the introduction of another body (internal body) inside a structure such as a container. The internal body is partially or completely submerged inside the structure. The convex domain of the fluid changes to a non-convex domain because of the internal body, whereas the fluid domain is simply connected and continuous. Evans and McIver (1987) explored the effect of introducing a vertical baffle into a rectangular container of water on fluid frequencies. The technique involved matching the appropriate eigenfunction expansions on either side of the baffle and the solution of the resulting integral equation for the horizontal fluid above or below the baffle. Watson and Evans (1991) extended this technique for a number of similar problems. Gavrilyuk et al. (2006) proposed fundamental solutions of the linearized problem on fluid sloshing in a vertical cylindrical container having a thin rigid-ring horizontal baffle. A pressure-based finite element technique has been developed to analyze the slosh dynamics of a partially filled rigid container with bottom-mounted submerged components by Mitra and Sinhamahapatra (2007). Maleki and Ziyaeifar (2008) investigated the potential of baffles (horizontal ring and vertical blade baffles) in increasing the hydrodynamic damping of sloshing in circular-cylindrical storage tanks. Cho et al. (2002) presented the fluid–structure interaction problems of fluid-storage containers with baffle, a disc-type baffle with an inner hole, by the structural-acoustic finite element formulation. Biswal et al. (2004) developed a finite element code and investigated the influence of a baffle, a thin annular circular plate, on the dynamic response of a partially fluid-filled cylindrical tank.

The previous problems in this class can be divided into two major categories. The first are those which considered the sloshing problem while the structure and internal body are assumed to be rigid, without considering any interaction between the fluid and the structure. The second category includes the works which considered the interaction between the fluid and the structure using numerical techniques. In spite of some achievements in the fluid–structure interaction problems, the problem as considered in the present paper has not been investigated so far. The main novelty of the present study is to propose a simple, robust, and efficient analytical method for investigating this class of problems including the interaction between the fluid and the structure. For brevity, the study is restricted to investigate the coupled vibration of a partially fluid-filled cylindrical container with an internal body. It is the first time that the effect of a cylindrical shell as internal body on vibration of fluid container is considered. The internal body has no contact with the container and is partially submerged inside the container, while the fluid domain is continuous, non-convex, and simply connected.

In the present paper, attention is focused on the bulging modes of the partially fluid-filled container without and with internal body. It can be noted that partially fluid-filled containers have two families of modes: sloshing and bulging ones (Amabili and Dalpiaz, 1998). Sloshing modes are caused by the oscillation of the fluid-free surface, whereas bulging modes are related to vibrations of the container walls (Amabili, 1999, 2000a; Koval'chuk and Fillin, 2003). In the present study, the effects of the free surface waves are neglected. In fact, it is well known that the effect of the free surface waves is low on bulging modes of structures which are not extremely flexible (Morand and Ohayon, 1995).

The boundary conditions are assumed to be clamped-free, and the Rayleigh–Ritz method is used to derive the characteristic equation of the container based on Love's thin shell theory. The internal body is a rigid, thin-walled, and open-ended cylindrical shell and is concentrically and partially submerged inside the container. The bottom plate of the container is assumed to be flat and rigid. Along the contact surface between the container and the fluid, the compatibility requirement is applied for the fluid–structure interactions. The fluid is assumed to be incompressible and inviscid. The velocity potential is formulated in terms of eigenfunction expansions appropriate to two distinct fluid regions which can be matched across their common vertical boundary. The resulting equations can be solved by using the Galerkin method. The validity of the proposed theoretical method for the partially water-filled cylindrical container without internal body is verified by comparing the results with those obtained from experimental and numerical solutions available in the literature. A finite element analysis is also used to check the validity of the present method for the partially water-filled cylindrical container with internal body. In order to evaluate the dynamic characteristics of the coupled system, the effects of the radius and length of the internal body and fluid level on the natural frequencies are also investigated.

2. Mathematical model

Consider a thin-walled cylindrical container of length L, radius a, and thickness t as shown in Fig. 1. The shell of the container is assumed to be made of an elastic material with Young's modulus E, Poisson ratio v, and mass density ρ_s. The bottom plate of the container is considered to be flat and rigid. The radial, circumferential, and axial coordinates are denoted by r, θ, and x, respectively. The container is filled to a height of H with an inviscid and incompressible fluid of mass density ρ_L. Another cylindrical shell is placed inside the container as internal body (Fig. 1). It is a thin-walled and open-ended rigid cylindrical shell of length h and radius b and is partially immersed in the container. The internal body thickness can be neglected in comparison to b and $(a-b)$.

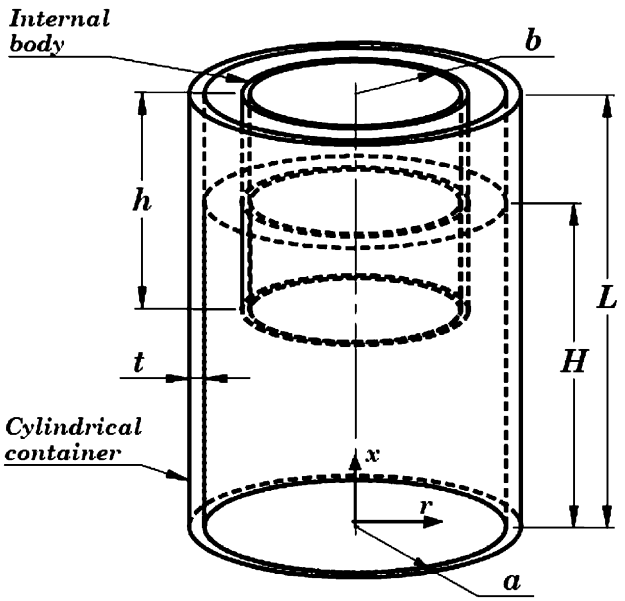

Fig. 1. Configuration of the internal body and the partially fluid-filled cylindrical container.

2.1. The cylindrical shell of the container

The potential energy for the thin isotropic cylindrical shell is given by (Kim et al., 2004; Soedel, 2003)

$$U_S = \frac{1}{2}\iint_{\Omega}\left[A_s\left(\varepsilon_x^2 + 2v\varepsilon_x\varepsilon_\theta + \varepsilon_\theta^2 + \frac{1-v}{2}\varepsilon_{x\theta}^2\right) + D_s\left(\kappa_x^2 + 2v\kappa_x\kappa_\theta + \kappa_\theta^2 + \frac{1-v}{2}\kappa_{x\theta}^2\right)\right] a\,\mathrm{d}x\,\mathrm{d}\theta, \tag{1}$$

$$A_s = \frac{Et}{1-v^2}, \quad D_s = \frac{Et^2}{12(1-v^2)}, \tag{2}$$

where coefficients A_s and D_s are stretching and bending stiffnesses of the shell, respectively. From Love's thin shell theory, the strain and curvature ε_i, κ_i, $i = x, \theta, x\theta$ in the middle surface are as follows (Kim et al., 2004; Soedel, 2003):

$$\begin{aligned}
&\varepsilon_x = \frac{\partial u}{\partial x}, \quad \varepsilon_\theta = \frac{1}{a}\left(\frac{\partial^2 w}{\partial\theta^2} + w\right), \quad \varepsilon_{x\theta} = \frac{1}{a}\frac{\partial u}{\partial\theta} + \frac{\partial v}{\partial x},\\
&\kappa_x = -\frac{\partial^2 w}{\partial x^2}, \quad \kappa_\theta = -\frac{1}{a^2}\left(\frac{\partial^2 w}{\partial\theta^2} - \frac{\partial v}{\partial\theta}\right), \quad \kappa_{x\theta} = -\frac{1}{a}\left(2\frac{\partial^2 w}{\partial x\,\partial\theta} - \frac{\partial v}{\partial x}\right),
\end{aligned} \tag{3}$$

where u, v, and w are axial, circumferential, and radial displacements of the shell of container on its middle surface, respectively.

The reference kinetic energy of the shell is given by (Kim et al., 2004; Soedel, 2003)

$$T_S^* = \frac{1}{2}\rho_s t\iint_{\Omega}[(u(x,\theta)^2 + v(x,\theta)^2 + w(x,\theta)^2]a\,\mathrm{d}x\,\mathrm{d}\theta. \tag{4}$$

The Rayleigh–Ritz method is applied to find natural modes of the partially fluid-filled container, and the time variation is assumed to be harmonic. The admissible displacement functions (Lee and Kim, 1999; Soedel, 2003) for free vibration of the cylindrical shell with any boundary conditions can be written as

$$\begin{aligned}
u(x,\theta) &= \sum_{s=1}^{\infty} U_{ns}\frac{1}{\alpha_s}\frac{\partial\Psi_s(x)}{\partial x}\cos(n\theta), \quad \alpha_s = \frac{\beta_s}{L},\\
v(x,\theta) &= \sum_{s=1}^{\infty} V_{ns}\Psi_s(x)\,\sin(n\theta),\\
w(x,\theta) &= \sum_{s=1}^{\infty} W_{ns}\Psi_s(x)\,\cos(n\theta),
\end{aligned} \tag{5}$$

where U_{ns}, V_{ns}, and W_{ns} are the parameters of the Ritz expansion, s and n are axial and circumferential mode numbers. $\Psi_s(x)$ is used as the axial mode that is the in vacuo beam function, satisfying the imposed boundary conditions.

In this article, the container with clamped-free boundary conditions (clamped at $x = 0$ and free at $x = L$) is considered. As a consequence, $\Psi_s(x)$ is given by

$$\Psi_s(x) = \left(\cosh\left(\frac{\beta_s x}{L}\right) - \cos\left(\frac{\beta_s x}{L}\right)\right) - \sigma_m\left(\sinh\left(\frac{\beta_s x}{L}\right) - \sin\left(\frac{\beta_s x}{L}\right)\right), \quad \sigma_m = \frac{\cosh(\beta_s) + \cos(\beta_s)}{\sinh(\beta_s) + \sin(\beta_s)}, \tag{6}$$

$$\cosh(\beta_s)\cos(\beta_s) + 1 = 0, \tag{7}$$

where β_s are solutions of Eq. (7).

2.2. Dynamic behavior of the fluid–structure interaction

The usual linearized theory of water wave permits the introduction of a velocity potential for the fluid motion. Assuming simple harmonic motion of radian frequency ω, the velocity potential can be expressed as

$$\tilde{\varphi}(r,\theta,x,t) = \mathrm{i}\omega\varphi(r,\theta,x)\,\mathrm{e}^{\mathrm{i}\omega t}, \quad \mathrm{i}^2 = -1. \tag{8}$$

In order to compute the time-independent velocity potential, $\varphi(r,\theta,x)$, the fluid domain (Evans and McIver, 1987; Watson and Evans, 1991) can be divided into two parts (I, II) as shown in Fig. 2

$$\mathrm{I} = \{(r,\theta,x) : r < b\} \text{ and } \mathrm{II} = \{(r,\theta,x) : b < r < a\}. \tag{9}$$

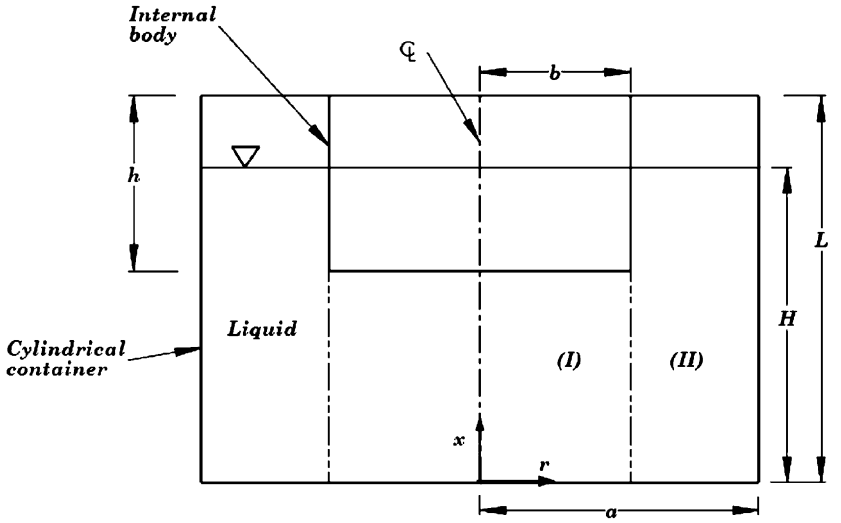

Fig. 2. Configuration of the partially fluid-filled cylindrical container in two dimensions.

The fluid deformation potential in two regions is assumed to be of the form below (Amabili, 1997b, 1999; Evans and McIver, 1987; Watson and Evans, 1991)

$$\varphi^{\mathrm{I}} = \sum_{s=1}^{\infty} W_{ns}\varphi_{ns}^{\mathrm{I}}, \quad \varphi^{\mathrm{II}} = \sum_{s=1}^{\infty} W_{ns}\varphi_{ns}^{\mathrm{II}}, \tag{10}$$

where φ^{I} and φ^{II} are time-independent velocity potentials and $\varphi_{ns}^{\mathrm{I}}$ and $\varphi_{ns}^{\mathrm{II}}$ are eigenfunctions in regions (I) and (II), respectively.

It is clear that we can restrict our attention to region (I), and seek function $\varphi^{\mathrm{I}}(r,\theta,x)$ that satisfies conditions (11)–(14) in that region, provided that at $r = 0$, φ^{I} is zero. so

$$\nabla^2\varphi^{\mathrm{I}} = 0, \tag{11}$$

$$\frac{\partial\varphi^{\mathrm{I}}}{\partial r} = 0 \quad \{r = b,\ L - h < x < H\}, \tag{12}$$

$$\frac{\partial\varphi^{\mathrm{I}}}{\partial x} = 0 \quad \{x = 0\}, \tag{13}$$

$$\frac{\mathrm{d}\tilde{\varphi}^{\mathrm{I}}}{\mathrm{d}t} = 0 \Rightarrow \varphi^{\mathrm{I}} = 0 \quad \{x = H\}, \tag{14}$$

where $\tilde{\varphi}^{\mathrm{I}}$ is velocity potential in region (I). This condition (14) states that the pressure on the free surface of the fluid in region (I) is zero.

For convenience we define

$$\gamma : [r = b, x < L - h], \quad \gamma' : [r = b, L - h < x < H], \tag{15}$$

where γ is the boundary between the two fluid regions and γ' is the contact boundary between the fluid and the internal body. In the inner fluid region (I), the method of separation of variables gives

$$\varphi_{ns}^{\mathrm{I}} = \cos(n\theta)\sum_{m=1}^{\infty} A_{mns}\cos(\lambda_m x) I_n(\lambda_m r), \quad \lambda_m = (2m-1)\frac{\pi}{2H} \tag{16}$$

which satisfies (11), (13), and (14) and also vanishes on $r = 0$ as required. I_n is the modified Bessel function of order n.

Now, we can restrict our attention to region (II), and seek function $\varphi^{\mathrm{II}}(r,\theta,x)$, satisfying conditions (17)–(21) in this region

$$\nabla^2\varphi^{\mathrm{II}} = 0, \tag{17}$$

$$\frac{\partial\varphi^{\mathrm{II}}}{\partial r} = 0 \quad \{r = b,\ L-h<x<H\}, \tag{18}$$

$$\frac{\partial\varphi^{\mathrm{II}}}{\partial x} = 0 \quad \{x = 0\}, \tag{19}$$

$$\frac{\mathrm{d}\tilde{\varphi}^{\mathrm{II}}}{\mathrm{d}t} = 0 \Rightarrow \varphi^{\mathrm{II}} = 0 \quad \{x = H\}, \tag{20}$$

where $\tilde{\varphi}^{\mathrm{II}}$ is velocity potential in region (II). This condition (20) states that the pressure on the free surface of the fluid in region (II) is zero

$$\frac{\partial\varphi^{\mathrm{II}}}{\partial r} = w \quad \{r = a,\ 0<x<H\}. \tag{21}$$

In the outer fluid region (II), the method of separation of variables gives

$$\varphi^{\mathrm{II}}_{ns} = \cos(n\theta)\sum_{m=1}^{\infty}\cos(\lambda_m x)[B_{mns}\mathrm{I}_n(\lambda_m r) + C_{mns}K_n(\lambda_m r)], \tag{22}$$

where C_{mns} and B_{mns} are unknown coefficients depending on the integer m, n, and s. K_n is the modified Bessel function of the second kind of order n. The function $\varphi^{\mathrm{II}}_{ns}$ satisfies the boundary conditions given in Eqs. (17), (19), and (20). Using Eq. (21) and eliminating $\cos(n\theta)$ leads to

$$\sum_{m=1}^{\infty}\cos(\lambda_m x)[B_{mns}I'_n(\lambda_m a) + C_{mns}K'_n(\lambda_m a)] = \Psi_s(x), \tag{23}$$

where I'_n and K'_n indicate the derivatives of I_n and K_n, with respect to r. Eq. (23) must be satisfied for all values, $0\leqslant x\leqslant H$. Multiplying this equation by $\cos(\lambda_j x)$ and then integrating between 0 and H, using the well-known properties of the orthogonal trigonometric functions, we obtain

$$C_{jns} = \frac{1}{K'_n(\lambda_j a)}\left\{\frac{2}{H}\int_0^H \Psi_s(x)\cos(\lambda_j x)\,\mathrm{d}x - B_{jns}I'_n(\lambda_j a)\right\}. \tag{24}$$

Here B_{jns} are unknown coefficients to be determined by the matching process. It is also necessary to ensure that the potentials and velocities of fluid are continuous along γ, and also the remaining conditions (12) and (18) are satisfied along γ'. These conditions can be written as follows:

$$\frac{\partial\varphi^{\mathrm{I}}}{\partial r}(r = b) = \left\{\begin{array}{cc} \dfrac{\partial\varphi^{\mathrm{II}}}{\partial r}(r = b) & \text{on } \gamma \\ 0 & \text{on } \gamma' \end{array}\right\}, \tag{25}$$

$$\varphi^{\mathrm{II}} = \varphi^{\mathrm{I}} \ \text{ on } \ \gamma, \tag{26a}$$

$$\frac{\partial\varphi^{\mathrm{II}}}{\partial r}(r = b) = 0 \ \text{ on } \ \gamma'. \tag{26b}$$

Eq. (25) must be satisfied for all values $0\leqslant x\leqslant H$ (on boundary, $\gamma+\gamma'$). After multiplying this equation by $\cos(\lambda_j x)$ and then integrating between 0 and H, we obtain the following equation:

$$A_{mns}\frac{H}{2}I'_n(\lambda_m b)\delta_{jm} = \sum_{m=1}^{\infty}[B_{mns}I'_n(\lambda_m b) + C_{mns}K'_{mns}(\lambda_m b)]\int_0^{L-h}\cos(\lambda_m x)\cos(\lambda_j x)\,\mathrm{d}x, \tag{27}$$

where δ_{jm} is the Kronecker delta function. Substituting C_{mns} from (25) in (27), the following systems of equations are obtained:

$$[\mathbf{A}_1]\{A_{ns}\} = [\mathbf{A}_2]\{B_{ns}\} + \{\mathbf{A}_3\}, \quad [\mathbf{A}_1]_{jm} = \frac{H}{2} I'_n(\lambda_m b)\delta_{jm}$$

$$[\mathbf{A}_2]_{jm} = \left[I'_n(\lambda_m b) - \frac{I'_n(\lambda_m a)}{K'_n(\lambda_m a)} K'_n(\lambda_m b) \right] \int_0^{L-h} \cos(\lambda_m x)\, \cos(\lambda_j x)\, \mathrm{d}x$$

$$\{\mathbf{A}_3\}_j = \sum_{m=1}^{\infty} \frac{2}{H} \frac{K'_n(\lambda_m b)}{K'_n(\lambda_m a)} \left(\int_0^H \Psi_s(x)\, \cos(\lambda_m x)\, \mathrm{d}x \right) \left(\int_0^{L-h} \cos(\lambda_m x)\, \cos(\lambda_j x)\, \mathrm{d}x \right)$$

$$A_{ns} = \begin{Bmatrix} A_{1ns} \\ \vdots \\ A_{mns} \end{Bmatrix}, \quad B_{ns} = \begin{Bmatrix} B_{1ns} \\ \vdots \\ B_{mns} \end{Bmatrix}. \tag{28}$$

Multiplying Eqs. (26a) and (26b) by $\cos(\lambda_j x)$ and then integrating along γ for (26a) and along γ' for (26b), gives

$$\sum_{m=1}^{\infty} \left[B_{mns} \left(I_n(\lambda_m b) - \frac{I'_n(\lambda_m a)}{K'_n(\lambda_m a)} K_n(\lambda_m b) \right) + \frac{2}{H} \frac{K_n(\lambda_m b)}{K'_n(\lambda_m a)} \right] \int_{L-h}^{H} \cos(\lambda_m x)\, \cos(\lambda_j x)\, \mathrm{d}x$$
$$+ \sum_{m=1}^{\infty} \left[B_{mns} \left(I'_n(\lambda_m b) - \frac{I'_n(\lambda_m a)}{K'_n(\lambda_m a)} K'_n(\lambda_m b) \right) + \frac{2}{H} \frac{K'_n(\lambda_m b)}{K'_n(\lambda_m a)} \int_0^H \Psi_s(x)\, \cos(\lambda_m x)\, \mathrm{d}x \right]$$
$$\times \int_0^{L-h} \cos(\lambda_m x)\, \cos(\lambda_j x)\, \mathrm{d}x = \sum_{m=1}^{\infty} A_{mns} I_n(\lambda_m b) \int_{L-h}^{H} \cos(\lambda_m x)\, \cos(\lambda_j x)\, \mathrm{d}x. \tag{29}$$

Eq. (29) can be written as

$$[\mathbf{B}_1]\{A_{ns}\} = [\mathbf{B}_2]\{B_{ns}\} + \{\mathbf{B}_3\}, \quad [\mathbf{B}_1]_{jm} = I_n(\lambda_m b) \int_{L-h}^{H} \cos(\lambda_m x)\, \cos(\lambda_j x)\, \mathrm{d}x,$$

$$[\mathbf{B}_2]_{jm} = \left(I_n(\lambda_m b) - \frac{I'_n(\lambda_m a)}{K'_n(\lambda_m a)} K_n(\lambda_m b) \right) \int_{L-h}^{H} \cos(\lambda_m x)\, \cos(\lambda_j x)\, \mathrm{d}x$$
$$+ \left(I'_n(\lambda_m b) - \frac{I'_n(\lambda_m a)}{K'_n(\lambda_m a)} K'_n(\lambda_m b) \right) \int_0^{L-h} \cos(\lambda_m x)\, \cos(\lambda_j x)\, \mathrm{d}x,$$

$$\{\mathbf{B}_3\}_j = \sum_{m=1}^{\infty} \left[\frac{K'_n(\lambda_m b)}{K'_n(\lambda_m a)} \int_{L-h}^{H} \cos(\lambda_m x) \cos(\lambda_j x)\, \mathrm{d}x + \frac{K_n(\lambda_m b)}{K'_n(\lambda_m a)} \int_0^{L-h} \cos(\lambda_m x)\, \cos(\lambda_j x)\, \mathrm{d}x \right] \frac{2}{H} \int_0^H \Psi_s(x)\, \cos(\lambda_m x)\, \mathrm{d}x,$$

$$A_{ns} = \begin{Bmatrix} A_{1ns} \\ \vdots \\ A_{mns} \end{Bmatrix}, \quad B_{ns} = \begin{Bmatrix} B_{1ns} \\ \vdots \\ B_{mns} \end{Bmatrix}. \tag{30}$$

The coefficients A_{mns} and B_{mns} are computed by solving the following system of equations:

$$\begin{cases} [\mathbf{A}_1]\{A_{ns}\} = [\mathbf{A}_2]\{B_{ns}\} + \{\mathbf{A}_3\}, \\ [\mathbf{B}_1]\{A_{ns}\} = [\mathbf{B}_2]\{B_{ns}\} + \{\mathbf{B}_3\}. \end{cases} \tag{31}$$

In order to calculate the natural frequencies and mode shapes, the Rayleigh–Ritz method is used. It is useful to introduce the Rayleigh quotient (Zhu, 1994; Amabili, 1997a, 2000b) for the systems considered, which is

$$\omega^2 = \frac{U_S}{T_S^* + T_L^*}, \tag{32}$$

where U_S and T_S^* are defined in Eqs. (1) and (4), respectively. The simplified reference kinetic energy of the fluid, T_L^*, is (Amabili, 1999)

$$T_L^* = \frac{1}{2} \rho_L \iint_{\Omega} \left(\varphi^{\mathrm{II}} \frac{\partial \varphi^{\mathrm{II}}}{\partial r} \right)_{r=a} a\, \mathrm{d}x\, \mathrm{d}\theta \tag{33}$$

by substituting Eq. (21) into Eq. (33), we can write

$$T_L^* = \frac{1}{2}\rho_L \int_0^{2\pi}\int_0^H \varphi^{\mathrm{II}}|_{r=a} wa\,\mathrm{d}x\,\mathrm{d}\theta. \tag{34}$$

2.3. The eigenvalue problem

For the numerical calculation of the natural frequencies and the parameters of the Ritz expansion of modes, only N terms in the expansion of u, v, and w (Eq. (5)), and M terms in the expansion of $\varphi_{ns}^{\mathrm{I}}$ and $\varphi_{ns}^{\mathrm{II}}$ (Eqs. (16) and (22)) are considered, where N and M are chosen large enough to give the required accuracy. So, all the energies are given by finite summations. It is convenient to introduce a vectorial notation. The vector $\mathbf{q}$ of the parameters of the Ritz expansion is defined by

$$\mathbf{q} = \begin{Bmatrix} \{U\} \\ \{V\} \\ \{W\} \end{Bmatrix}, \quad \{U\} = \begin{Bmatrix} U_{n1} \\ \vdots \\ U_{ns} \end{Bmatrix}, \quad \{V\} = \begin{Bmatrix} V_{n1} \\ \vdots \\ V_{ns} \end{Bmatrix}, \quad \{W\} = \begin{Bmatrix} W_{n1} \\ \vdots \\ W_{ns} \end{Bmatrix}. \tag{35}$$

The maximum potential energy of the shell (Eq. (1)), becomes

$$U_S = \tfrac{1}{2}\pi \mathbf{q}^{\mathrm{T}}\mathbf{K}_s\mathbf{q}, \tag{36}$$

the partitioned matrix $\mathbf{K}_s$ is

$$\mathbf{K}_s = \begin{bmatrix} [\mathbf{K}_{11}] & [\mathbf{K}_{12}] & [\mathbf{K}_{13}] \\ [\mathbf{K}_{12}]^{\mathrm{T}} & [\mathbf{K}_{22}] & [\mathbf{K}_{23}] \\ [\mathbf{K}_{13}]^{\mathrm{T}} & [\mathbf{K}_{23}]^{\mathrm{T}} & [\mathbf{K}_{33}] \end{bmatrix}, \tag{37}$$

where the elements of the submatrices $[\mathbf{K}_{ij}]$ $(i,j = 1,2,3)$ are given by

$$\begin{aligned}
[\mathbf{K}_{11}]_{ij} &= \frac{A_s}{\alpha_i\alpha_j}\left[a\int_0^L \frac{\partial^2\Psi_i}{\partial x^2}\frac{\partial^2\Psi_j}{\partial x^2}\,\mathrm{d}x + (1-v)\frac{n^2}{2a}\int_0^L \frac{\partial\Psi_i}{\partial x}\frac{\partial\Psi_j}{\partial x}\,\mathrm{d}x\right],\\
[\mathbf{K}_{12}]_{ij} &= \frac{A_s n}{2\alpha_i}\left[-2v\int_0^L \frac{\partial^2\Psi_i}{\partial x^2}\Psi_j\,\mathrm{d}x + (1-v)\int_0^L \frac{\partial\Psi_i}{\partial x}\frac{\partial\Psi_j}{\partial x}\,\mathrm{d}x\right], \quad K_{13}(i,j) = -\frac{A_s v}{\alpha_i}\int_0^L \frac{\partial^2\Psi_i}{\partial x^2}\Psi_j\,\mathrm{d}x,\\
[\mathbf{K}_{22}]_{ij} &= \left(A_s a\frac{1-v}{2} + D_s\frac{1-v}{2a}\right)\int_0^L \frac{\partial\Psi_i}{\partial x}\frac{\partial\Psi_j}{\partial x}\,\mathrm{d}x + \left(D_s\frac{n^2}{a^3} + A_s\frac{n^2}{a}\right)\int_0^L \Psi_i\Psi_j\,\mathrm{d}x,\\
[\mathbf{K}_{23}]_{ij} &= \left(A_s\frac{n}{a} + D_s\frac{n^3}{a^3}\right)\int_0^L \Psi_i\Psi_j\,\mathrm{d}x + D_s\left[n\left(\frac{1-v}{a}\int_0^L \frac{\partial\Psi_i}{\partial x}\frac{\partial\Psi_j}{\partial x}\,\mathrm{d}x - \frac{v}{a}\int_0^L \frac{\partial^2\Psi_i}{\partial x^2}\Psi_j\,\mathrm{d}x\right)\right],\\
[\mathbf{K}_{33}]_{ij} &= \frac{A_s}{a}\int_0^L \Psi_i\Psi_j\mathrm{d}x + D_s\left[a\int_0^L \frac{\partial^2\Psi_i}{\partial x^2}\frac{\partial^2\Psi_j}{\partial x^2}\,\mathrm{d}x + 2v\frac{n^2}{a}\int_0^L \frac{\partial^2\Psi_i}{\partial x^2}\Psi_j\,\mathrm{d}x + \frac{n^4}{a^3}\int_0^L \Psi_i\Psi_j\,\mathrm{d}x + 2n^2\frac{1-v}{a}\int_0^L \frac{\partial\Psi_i}{\partial x}\frac{\partial\Psi_j}{\partial x}\,\mathrm{d}x\right].
\end{aligned} \tag{38}$$

The reference kinetic energy of the shell (Eq. (4)), can be written as

$$T_S^* = \tfrac{1}{2}\pi \mathbf{q}^{\mathrm{T}}\mathbf{M}_s\mathbf{q}, \tag{39}$$

where

$$\mathbf{M}_s = \begin{bmatrix} [\mathbf{M}_{11}] & [\mathbf{0}] & [\mathbf{0}] \\ [\mathbf{0}] & [\mathbf{M}_{22}] & [\mathbf{0}] \\ [\mathbf{0}] & [\mathbf{0}] & [\mathbf{M}_{33}] \end{bmatrix}, \tag{40}$$

where the elements of the submatrices $[\mathbf{M}_{ii}]$ $(i = 1,2,3)$ are given by

$$[\mathbf{M}_{11}]_{ij} = a\rho_s t\int_0^L \frac{\partial\Psi_i}{\alpha_i\,\partial x}\frac{\partial\Psi_j}{\alpha_j\partial x}\,\mathrm{d}x, \quad [\mathbf{M}_{22}]_{ij} = [\mathbf{M}_{33}]_{ij} = a\rho_s t\int_0^L \Psi_i(x)\Psi_j(x)\,\mathrm{d}x. \tag{41}$$

The simplified reference kinetic energy of the fluid (Eq. (34)), can be written as

$$T_L^* = \tfrac{1}{2}\pi \mathbf{q}^{\mathrm{T}} \mathbf{M}_L \mathbf{q}, \tag{42}$$

where

$$\mathbf{M}_L = \begin{bmatrix} [\mathbf{0}] & [\mathbf{0}] & [\mathbf{0}] \\ [\mathbf{0}] & [\mathbf{0}] & [\mathbf{0}] \\ [\mathbf{0}] & [\mathbf{0}] & [\mathbf{M}_F] \end{bmatrix} \tag{43}$$

in which the elements of submatrix $[\mathbf{M}_F]$ can be written as

$$[\mathbf{M}_F]_{ij} = a\rho_L \sum_{m=1}^{M} \int_0^H \cos(\lambda_m x)\Psi_j(x)\,\mathrm{d}x \left(B_{mni}\left(I_n(\lambda_m a) - \frac{I_n'(\lambda_m a)}{K_n'(\lambda_m a)} K_n(\lambda_m a) \right) + \frac{2}{H} \frac{K_n(\lambda_m a)}{K_n'(\lambda_m a)} \int_0^H \Psi_i(x)\cos(\lambda_m x)\,\mathrm{d}x \right). \tag{44}$$

Substituting Eqs. (36), (39), and (42) into the Rayleigh quotient (Eq. (32)), and then minimizing with respect to the coefficients $\mathbf{q}_i$, we obtain

$$\mathbf{K}_s \mathbf{q} - \omega^2 (\mathbf{M}_s + \mathbf{M}_L)\mathbf{q} = 0, \tag{45}$$

where ω is the circular frequency of the container partially filled with fluid. Eq. (45) gives a linear eigenvalue problem for a real, non-symmetric matrix.

3. Results and discussion

Based on the preceding analysis, the eigenvalue problem (Eq. (45)), is solved to find the natural frequencies and mode shapes of a partially fluid-filled cylindrical container with and without internal body. To check the validity and accuracy of the proposed method, the comparisons are made with experimental and FEM results. In the finite element analysis, the two-dimensional axisymmetric model is constructed with the axisymmetric structural shell element for elastic structure and axisymmetric fluid element for the fluid region. Shell element is defined by two nodes having four degrees of freedom at each node: three translations in each direction and one rotation. Fluid element is defined by four nodes having three degrees of freedom at each node: three translations in each direction (Zienkiewicz, 1977). The radial velocities of the fluid nodes along the wet surface of the container coincide with the corresponding velocities of the container. The radial velocities of the fluid nodes along the wet surface of the internal body are zero. In the present paper, the effects of the free surface waves are neglected; consequently, the time-independent velocity potential $\varphi(r,\theta,x)$, of the fluid nodes on the free surface in two regions (I, II) is zero.

The following material properties are used: the container is made of steel with Young's modulus $E = 206\,\mathrm{GPa}$, Poisson's ratio $\nu = 0.3$, and mass density $\rho_s = 7850\,\mathrm{kg/m^3}$; the fluid is water with mass density $\rho_L = 1000\,\mathrm{kg/m^3}$.

3.1. Convergence study

To check the convergence of the proposed method, a partially water-filled container with a cylindrical shell as an internal body and clamped-free boundary conditions is analyzed. This container is partially filled to $H = 0.67L$ and its dimensions are $a = 0.2$, $b = 0.85a$, $L = 3a$, $h = 0.67L$, and $t = 0.002$. Tables 1 and 2 show the convergence of the proposed method for different number of terms used in the series expansions. From the frequencies presented in these tables, we conclude that just 15 terms in the series expansions are adequate for convergence.

To validate the proposed theoretical method, the results for a partially water-filled cylindrical container with and without internal body are compared with those obtained from the finite element analysis, in Table 3. The agreement between the results is very good and the maximum differences are less than 2% and 4.6% for a partially water-filled cylindrical container without and with internal body, respectively.

The uncoupled modes and associated frequencies of a partially water-filled clamped-free cylindrical container without internal body are also obtained by solving the eigenvalue problem (Eq. (45)). The results of the present study are compared with the experimental measurements and finite element calculations (Mazúch et al., 1996), in Table 4. Here, the cylindrical container has a length of $L = 0.231$, radius $a = 0.07725$, and thickness $t = 0.0015$. The container is made of steel, and has the material properties: Young's modulus $E = 205\,\mathrm{GPa}$, Poisson's ratio $\nu = 0.3$, and mass density $\rho_s = 7800\,\mathrm{kg/m^3}$. The fluid is water with mass density $\rho_L = 1000\,\mathrm{kg/m^3}$. For the first 10 modes, the predicted

Table 1
Convergence study of natural frequencies (Hz), effect of the series terms N with $M = 15$.

Mode		N					
n	m	2	6	10	14	15	16
2	1	206.12	198.04	196.48	195.82	195.71	195.62
	2	719.7	674.34	665.04	662.16	661.93	661.7
3	1	135.3	132.05	131.39	131.12	131.1	131.09
	2	485.82	433.77	429.14	427.67	427.54	427.46
4	1	154.61	152.4	152	151.86	151.85	151.85
	2	357.97	332.19	329.8	329.03	328.95	328.89
5	1	213.09	208.94	208.49	208.33	208.32	208.31
	2	354.56	338.61	337.33	336.9	336.84	336.81
6	1	284.29	276.89	276.52	276.38	276.37	276.37
	2	450.5	426.89	425.42	424.92	424.83	424.75

Table 2
Convergence study of natural frequencies (Hz), effect of the series terms M with $N = 15$.

Mode		M				
n	m	5	10	15	20	22
2	1	188.64	184.44	195.62	194.18	194.63
	2	639.23	623.77	661.7	656.55	658.25
3	1	129.4	127.23	131.1	130.54	130.65
	2	414.36	409.23	427.54	424.55	425.18
4	1	150.99	149.67	151.85	151.37	151.45
	2	323	320.94	328.95	327.43	327.74
5	1	206.81	205.3	208.32	207.58	207.86
	2	335.2	333.78	336.84	336.11	336.59
6	1	274.34	272.98	276.37	275.45	275.97
	2	425.76	422.94	424.83	424.12	424.48

frequencies show good agreement with the experimental and numerical data of Mazúch et al. (1996). However, there are some differences between the results. These differences are not more than 3.9% in comparison with the experiment data, except for the mode shape ($m = 1$ and $n = 2$), and 4.6% when compared with the finite element results. For the mode shape ($m = 1$ and $n = 2$), there is approximately 15% difference between the present results and the experimental measurements for all filling ratios. Mazúch et al. (1996) also observed a similar discrepancy between their predictions and the experimental measurements for the above-mentioned mode shape ($m = 1$ and $n = 2$) (see Table 4). These discrepancies may be due to the sensitivity of the lower order modes to the boundary conditions existing in the experiment. It was also reported by Mazúch et al. (1996) that the end of the cylindrical shell at the base was, probably, not so perfectly fixed in the experiment as was supposed in the finite element model.

Table 3
Coupled natural frequencies (Hz) of a partially fluid-filled cylindrical container without/with internal body.

Mode	Without internal body		With internal body	
	FEM	This study	FEM	This study
1st	145.63(1,3)	146.07(1,3)	128.63(1,3)	131.1(1,3)
2nd	164.55(1,4)	165.07(1,4)	146.9(1,4)	151.85(1,4)
3rd	225.7(1,5)	225.49(1,5)	193.77(1,2)	195.71(1,2)
4th	225.97(1,2)	228.8(1,2)	199.05(1,5)	208.32(1,5)
5th	288.09(1,6)	293.83(1,6)	264.93(1,6)	276.37(1,6)
6th	335.81(2,5)	341.09(2,5)	321.22(2,4)	328.95(2,4)
7th	337.14(2,4)	343.5(2,4)	327.75(2,5)	336.84(2,5)

Table 4
Coupled natural frequencies (Hz) of a partially fluid-filled cylindrical container without internal body, compared with Mazúch et al. (1996).

Mode	Partially fluid-filled cylindrical container							
	$H/L=0.5$		$H/L=0.7$			$H/L=1$		
(m,n)	This study	FEM	This study	FEM	Exp.	This study	FEM	Exp.
(1,3)	612	609.4	542.2	543.1	522	398.9	400.6	388
(1,2)	771.27	771.1	669.7	672.7	582	478.8	482.1	421
(1,4)	906.82	908.8	796.2	806.0	798	627.5	633.2	628
(1,5)	1311.7	1352.8	1151.6	1188.4	1196	1015.6	1033.0	1027
(2,4)	1280.1	1303.9	1239	1253.2	1244	1078.7	1110.6	1094
(1,1)	1659.6	1654.4	1405.8	1407.4	–	1035.4	1038.6	–
(2,5)	1555.2	1565.8	1534.5	1553.8	1546	1251.6	1304.2	1299
(2,3)	1508.5	1515.2	1422.2	1425.3	1394	1272.8	1286.9	1254
(1,6)	1757.4	1842.7	1616	1679.7	–	1524.2	1561.3	1546
(2,6)	2179.4	2189.0	2035.6	–	–	1681.1	1762.6	1748

3.2. Effect of fluid level

In order to study the effect of the fluid level on the natural frequencies of a partially fluid-filled cylindrical container without and with internal body, a normalized natural frequency is defined as f_2/f_1, where f_1 and f_2 stand for the natural frequencies of the empty and the partially fluid-filled container for the specific corresponding mode, respectively.

Fig. 3 shows the predicted natural frequencies of the partially water-filled cylindrical container as a function of filling ratio (H/L) for various circumferential and axial mode numbers. From Fig. 3, it is seen that the frequencies decrease with increasing filling ratio (H/L). For a specific circumferential and axial mode numbers, the frequency variations are very similar for the partially fluid-filled container with and without internal body. But, the effect of the fluid level on the natural frequencies for the partially water-filled container without internal body is less than the effect of the fluid level on the natural frequencies for the fluid container with internal body. The natural frequencies of a completely fluid-filled cylindrical container decrease by 60%, compared to those of empty container. For the axial mode number ($m=1$), the effect of the fluid level is very small in lower filling ratios ($H/L<0.4$). The effect of the fluid on the frequencies of the partially fluid-filled container is stronger for modes with smaller circumferential and axial mode numbers n, m. This conclusion is in agreement with the results obtained by Koval'chuk and Kruk (2006). As can be seen from Fig. 3, the variations of the natural frequencies with fluid level also depend on the axial and circumferential mode numbers.

3.3. Effect of internal body radius

Fig. 4 shows the calculated natural frequencies of the partially water-filled cylindrical container as a function of radius ratio b/a, for various circumferential and axial mode numbers. It is observed from Fig. 4 that the normalized

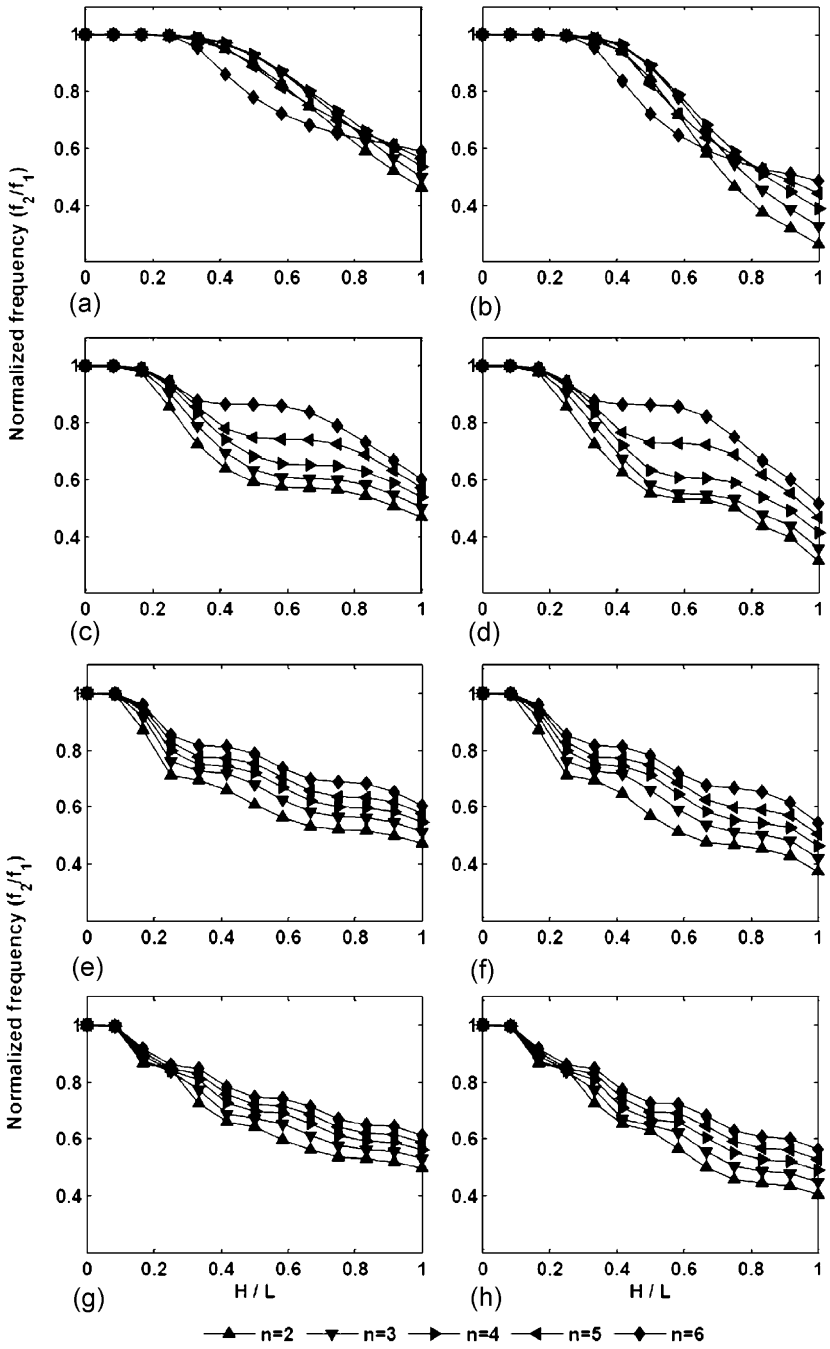

Fig. 3. Effect of fluid level on natural frequencies for the partially fluid-filled container: (a) first axial mode ($m = 1$) without internal body, (b) first axial mode ($m = 1$) with internal body, (c) second axial mode ($m = 2$) without internal body, (d) second axial mode ($m = 2$) with internal body, (e) third axial mode ($m = 3$) without internal body, (f) third axial mode ($m = 3$) with internal body, (g) fourth axial mode ($m = 4$) without internal body, and (h) fourth axial mode ($m = 4$) with internal body.

natural frequencies decrease with increasing radius ratio (b/a). The effect of internal body radius on the frequencies of the partially fluid-filled container is stronger for modes with smaller circumferential mode numbers n. The normalized natural frequencies of the partially water-filled cylindrical container with radius ratio $b/a = 0.95$ decrease about 40%, compared to those of the fluid container without internal body where the maximum reduction is for the axial mode

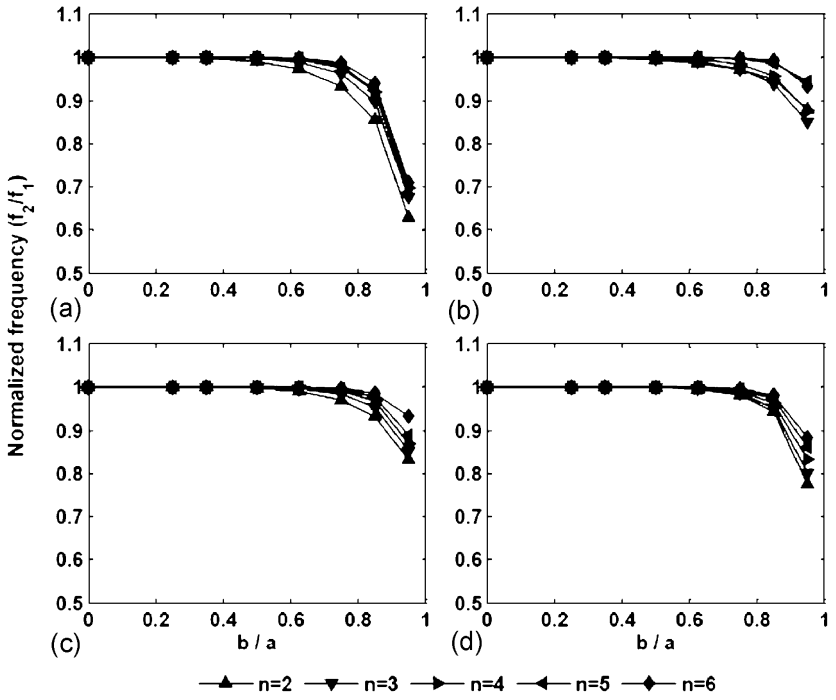

Fig. 4. Natural frequencies of the partially fluid-filled container as a function of radius ratio (b/a): (a) first axial mode ($m = 1$), (b) second axial mode ($m = 2$), (c) third axial mode ($m = 3$), and (d) forth axial mode ($m = 4$) (f_1 and f_2 stand for the natural frequencies of the partially fluid-filled container without and with internal body for the specific corresponding mode, respectively).

number $m = 1$. As can be seen from Fig. 4, the variations of the natural frequencies with radius ratio also depend on the axial and circumferential mode numbers.

The wide-spacing approximation has proved a remarkably accurate tool for solving radiation and scattering problems in water waves when more than one body is involved (Watson and Evans, 1991). The method is based on the assumption that the bodies are sufficiently widely spaced for the local wave-field in the vicinity of one body not affecting the others. It has been used by Ohkusu (1970) to consider the problem of two half-immersed cylinders and Srokosz and Evans (1979) who considered two rolling plates. Now, as seen in Fig. 4, for the radius ratio $0 < b/a < 0.5$, the internal body has no effect on the natural frequencies of the fluid container. This indicates a good agreement between the present method and the wide-spacing approximation.

3.4. Effect of internal body length

Fig. 5 shows the normalized natural frequencies of the partially water-filled cylindrical container as a function of length ratio h/L, for various circumferential and axial mode numbers. As can be observed from Fig. 5, the natural frequencies decrease with increasing length ratio. Consequently, the minimum frequencies are obtained when the fluid domain is completely divided into two parts $h/L = 1$. The effect of internal body length on the natural frequencies of the partially fluid-filled container is stronger for modes with smaller circumferential mode numbers n. The normalized natural frequencies of the partially fluid-filled container with length ratio ($h/L = 1$) decrease about 25%, compared to those of the fluid container without internal body. As can be seen from Fig. 5, the variations of the natural frequencies with length ratio also depend on the axial and circumferential mode numbers.

3.5. Vibration mode shapes

The first four mode shapes having $n = 2$ are shown in Fig. 6. Mode shapes are plotted for the container section defined by $\theta = 0$ and π. Obviously, the mode shapes are symmetric in this case. The natural frequencies of the

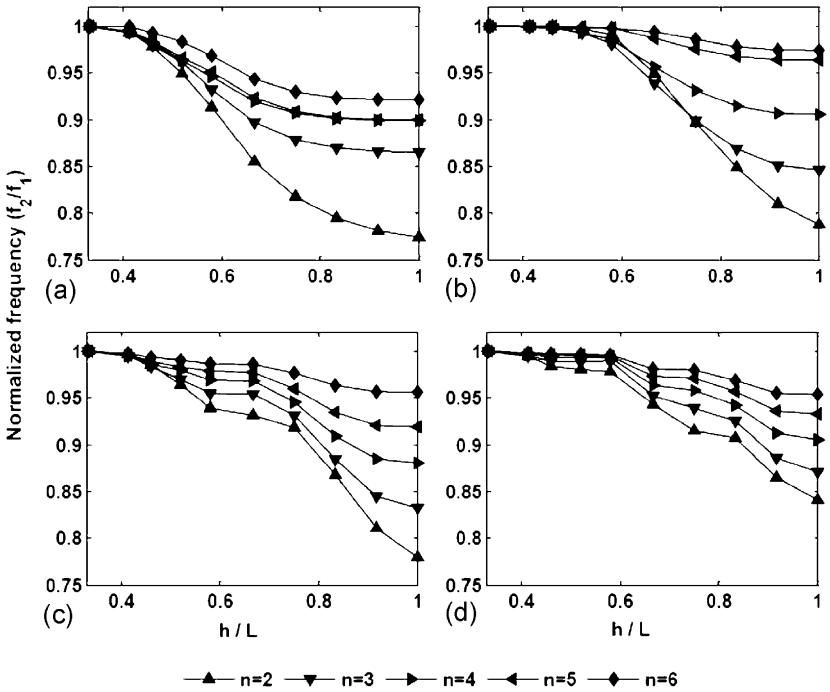

Fig. 5. Natural frequencies of the partially fluid-filled container as a function of length ratio h/L: (a) first axial mode ($m = 1$), (b) second axial mode ($m = 2$), (c) third axial mode ($m = 3$), and (d) fourth axial mode ($m = 4$) (f_1 and f_2 stand for the natural frequencies of the partially fluid-filled container without and with internal body for the specific corresponding mode, respectively).

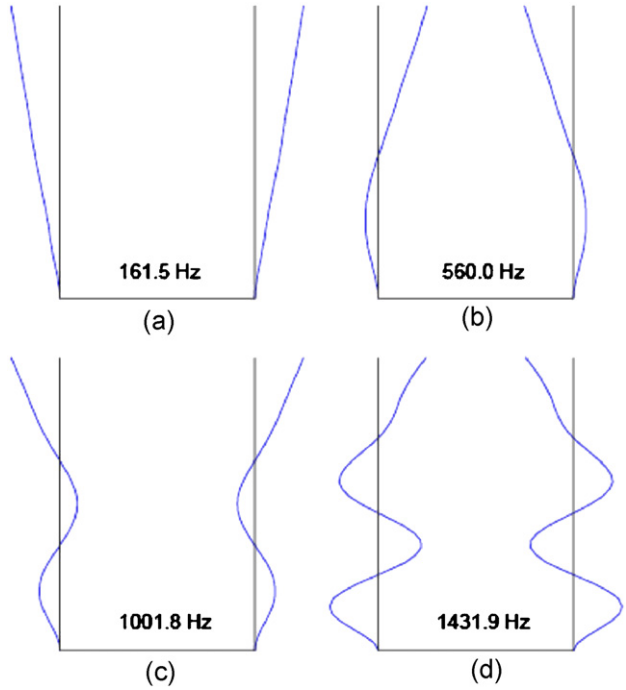

Fig. 6. First four modes having $n = 2$ (circumferential wave number) for the partially fluid-filled container with internal body and their natural frequencies. The corresponding natural frequencies (without internal body) are: (a) 230.9 Hz, (b) 705.0 Hz, (c) 1255.2 Hz, and (d) 1706.7 Hz.

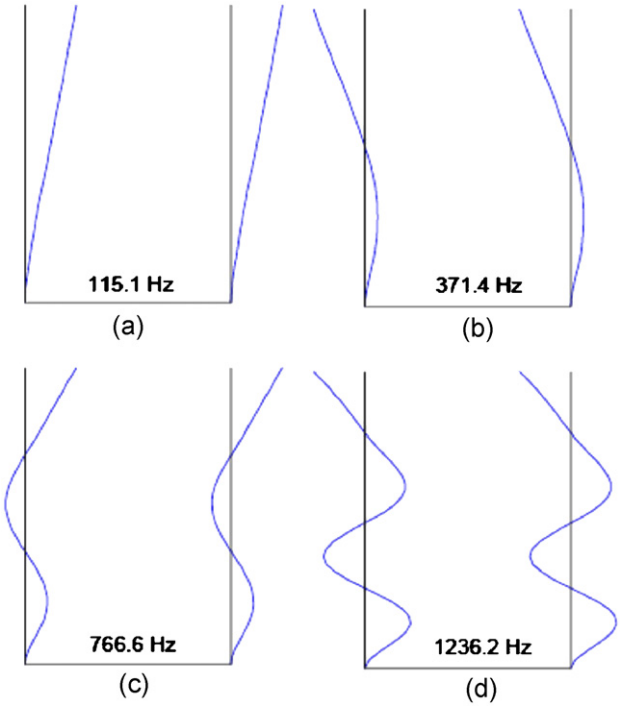

Fig. 7. First four modes having $n = 3$ (circumferential wave number) for the partially fluid-filled container and their natural frequencies. The corresponding natural frequencies (without internal body) are: (a) 146.8 Hz, (b) 459.2 Hz, (c) 946.4 Hz, and (d) 1436.5 Hz.

corresponding modes for the fluid container without internal body are also given in the caption to evaluate the effect of the internal body. The first four mode shapes having $n = 3$ are presented in Fig. 7. The modes are antisymmetric in this case.

4. Conclusions

Pursuing an analytically oriented method to consider the effects of a rigid internal body on the coupled vibration of a partially fluid-filled cylindrical container, we developed a robust and efficient approach which captures the analytical features of velocity potential in a continuous, simply connected, and non-convex fluid domain. It has many advantages over traditional numerical schemes. Another very important advantage of this method is the possibility of testing and analyzing numerous sizes of internal bodies within the container and, therefore, of drawing the necessary physical and engineering conclusions.

In order to evaluate the dynamic characteristics of the fluid-coupled system, the effects of fluid level, internal body radius, and internal body length on the natural frequencies were investigated. It was found that the increase of internal body radius decreases the natural frequencies of the partially water-filled container. Also, the natural frequency of the partially water-filled container decreases as the length ratio increases. The effects of fluid level, internal body radius, and internal body length on the frequencies of the partially water-filled container vary with the mode numbers (n, m), i.e., this effect is stronger for modes with smaller circumferential and axial mode numbers.

The proposed analytical method was verified by experimental and numerical data and the results showed excellent agreement. This method can also be extended to the fluid–structure interaction problems involving internal bodies with different shapes.

References

Amabili, M., 1996. Comments on "Rayleigh–Ritz method in coupled fluid–structure interacting systems and its applications". Journal of Sound and Vibration 195, 346–347.

Amabili, M., 1997a. Ritz method and substructuring in the study of vibration with strong fluid–structure interaction. Journal of Fluids and Structures 11, 507–523.
Amabili, M., 1997b. Shell–plate interaction in the free vibrations of circular cylindrical tanks partially filled with a liquid: the artificial spring method. Journal of Sound and Vibration 199, 431–452.
Amabili, M., 1999. Vibrations of circular tubes and shells filled and partially immersed in dense fluids. Journal of Sound and Vibration 221 (4), 567–585.
Amabili, M., 2000a. Eigenvalue problems for vibrating structures coupled with quiescent fluids with free surface. Journal of Sound and Vibration 231 (1), 79–97.
Amabili, M., 2000b. Vibrations of fluid-filled hermetic cans. Journal of Fluids and Structures 14, 235–255.
Amabili, M., Dalpiaz, G., 1998. Vibrations of base plates in annular cylindrical tanks: theory and experiments. Journal of Sound and Vibration 210 (3), 329–350.
Amabili, M., Paidoussis, M.P., Lakis, A.A., 1998. Vibrations of partially filled cylindrical tanks with ring-stiffeners and flexible bottom. Journal of Sound and Vibration 213, 259–299.
Bauer, H.F., Komatsu, K., 1994. Coupled frequencies of a hydroelastic system of an elastic two-dimensional sector-shell and frictionless liquid in zero gravity. Journal of Fluids and Structures 8, 817–831.
Biswal, K.C., Bhattacharyya, S.K., Sinha, P.K., 2004. Dynamic response analysis of a fluid-filled cylindrical tank with annular baffle. Journal of Sound and Vibration 274, 13–37.
Cheung, Y.K., Zhou, D., 2002. Hydroelastic vibration of a circular container bottom plate using the Galerkin method. Journal of Fluids and Structures 16 (4), 561–580.
Cho, J.R., Lee, H.W., Kim, K.W., 2002. Free vibration analysis of baffled liquid-storage tanks by the structural-acoustic finite element formulation. Journal of Sound and Vibration 258 (5), 847–866.
Ergin, A., Temarel, P., 2002. Free vibration of a partially fluid-filled and submerged horizontal cylindrical shell. Journal of Sound and Vibration 254 (5), 951–965.
Evans, D.V., McIver, P., 1987. Resonant frequencies in a container with a vertical baffle. Journal of Fluid Mechanics 175, 295–307.
Gavrilyuk, I., Lukovsky, I., Trotsenko, Yu., Timokha, A., 2006. Sloshing in a vertical circular cylindrical tank with an annular baffle. Part 1. Linear fundamental solutions. Journal of Engineering Mathematics 54, 71–88.
Jadic, I., So, R.M.C., Mignolet, M.P., 1998. Analysis of fluid–structure interactions using a time-merching technique. Journal of Fluids and Structures 12, 631–654.
Jeong, K.H., 2006. Hydroelastic vibration of two annular plates coupled with a bounded compressible fluid. Journal of Fluids and Structures 22, 1079–1096.
Jeong, K.H., Lee, S.C., 1998. Hydroelastic vibration of a liquid-filled circular cylindrical shell. Computers and Structures 66, 173–185.
Kim, Y.W., Lee, Y.S., Ko, S.H., 2004. Coupled vibration of partially fluid-filled cylindrical shells with ring stiffeners. Journal of Sound and Vibration 276, 869–897.
Kondo, H., 1981. Axisymmetric vibration analysis of a circular cylindrical tank. Bulletin of the Japan Society of Mechanical Engineers 24, 215–221.
Koval'chuk, P.S., Fillin, V.G., 2003. On modes of flexural vibrations of initially bent cylindrical shells partially filled with a liquid. International Applied Mechanics 39 (4), 464–471.
Koval'chuk, P.S., Kruk, L.A., 2006. On the spectrum of natural frequencies of circular cylindrical shells completely filled with a fluid. International Applied Mechanics 42 (5), 529–535.
Krishna, B.V., Ganesan, N., 2007. Studies on fluid-filled and submerged cylindrical shells with constrained viscoelastic layer. Journal of Sound and Vibration 303, 575–595.
Lee, Y.S., Kim, Y.W., 1999. Effect of boundary conditions on natural frequencies for rotating composite cylindrical shells with orthogonal stiffeners. Advances in Engineering Software 30, 649–655.
Maleki, A., Ziyaeifar, M., 2008. Sloshing damping in cylindrical liquid storage tanks with baffles. Journal of Sound and Vibration 311, 372–385.
Mazúch, T., Horaček, J., Trnka, J., Veselý, J., 1996. Natural modes and frequencies of a thin clamped–free steel cylindrical storage tank partially filled with water: FEM and measurements. Journal of Sound and Vibration 193, 669–690.
Mikami, T., Yoshimura, J., 1992. The collocation method for analyzing free vibration of shells of revolution with either internal or external fluids. Computers and Structures 44, 343–351.
Mitra, S., Sinhamahapatra, K.P., 2007. Slosh dynamics of liquid-filled containers with submerged components using pressure-based finite element method. Journal of Sound and Vibration 304, 361–381.
Morand, H.J.P., Ohayon, R., 1995. Fluid–structure Interaction. Applied Numerical Methods. Wiley, New York.
Ohkusu, M., 1970. Hydrodynamic forces on multiple cylinders in waves. In: Proceedings of the International Symposium on Dynamics of Marine Vehicles and Structures in Waves, London, pp. 107–112.
Soedel, W., 2003. Vibrations of Shells and Plates. Marcel Dekker, New York.
Srokosz, M.A., Evans, D.V., 1979. A theory for wave-power absorption by two independently oscillating bodies. Journal of Fluid Mechanics 90, 337–362.
Watson, E.B.B., Evans, D.V., 1991. Resonant frequencies of a fluid in containers with internal bodies. Journal of Engineering Mathematics 25, 115–135.
Yamaki, N., Tani, J., Yamaji, T., 1984. Free vibration of a clamped–clamped circular cylindrical shell partially filled with fluid. Journal of Sound and Vibration 94, 531–550.

Zhu, F., 1994. Rayleigh quotients for coupled free vibrations. Journal of Sound and Vibration 171, 641–649.
Zhu, F., 1995. Rayleigh–Ritz method in coupled fluid–structure interacting systems and its applications. Journal of Sound and Vibration 186, 543–550.
Zienkiewicz, O.C., 1977. The Finite Element Method. McGraw-Hill Company, London.